Experimental Laboratory Research

Monitoring of Short-Term Erythropoietin Therapy in Rats with Acute Spinal Cord Injury Using Manganese-Enhanced Magnetic Resonance Imaging

Martin Thomas Freitag, MD, Gábor Márton, MSc, Krisztián Pajer, MSc, Jens Hartmann, MD, Nadja Walder, MD, Markus Rossmann, MD, Peter Parzer, MSc, Heinz Redl, PhD, Antal Nógrádi, MD, PhD, DSc*, Bram Stieltjes, MD, PhD*

From the Quantitative Imaging-Based Disease Characterization, Department of Radiology, German Cancer Research Center (DKFZ), Heidelberg, Germany (MTF, BS); Laboratory of Neural Regeneration, Department of Anatomy, Histology, and Embryology, Faculty of Medicine, University of Szeged, Hungary (GM, KP, AN); Ludwig Boltzmann Institute for Experimental and Clinical Traumatology, Research Center of the AUVA, Vienna, Austria (JH, NW, MR, HR, AN); and Section Disorders of Personality Development, Department of Child and Adolescent Psychiatry, Center for Psychosocial Medicine, University of Heidelberg, Germany (PP).

ABSTRACT

BACKGROUND AND PURPOSE

To evaluate the short-term outcome of erythropoietin (EPO) therapy in rats with spinal cord injury (SCI) using manganese-enhanced magnetic resonance imaging (MEMRI).

METHODS

Rats were divided in an EPO and a control group. Laminectomy at Th11 was performed, followed by SCI. $MnCl_2$ was applied into the cisterna magna and functional recovery was examined after injury using BBB-scoring. Then, rats were euthanized and the spinal cord was extracted for MEMRI. Finally, histological analysis was performed and correlated with MEMRI.

RESULTS

EPO-treated animals showed significantly better functional recovery ($P = .008$, $r = .62$) and higher mean signal-to-noise ratio (SNR) in MEMRI compared to controls for slices 10-13 ($P = .017$, $R^2 = .31$) at the level of the lesion epicenter. Functional recovery correlated significantly with higher SNR values, determined using the mean SNR between slices 10 and 13 ($P = .047$, $R^2 = .36$). In this region, histology revealed a significantly decreased number of microglia cells and apoptosis in EPO-treated animals.

CONCLUSION

MEMRI successfully depicts the therapeutic effect of EPO in early SCI that leads to a significant recovery in rats, a significantly reduced immune response and significantly reduced number of apoptotic cells at the height of the lesion epicenter.

Keywords: Neuroprotection, neuroregeneration, apoptosis, inflammation, EPO, spinal cord injury.

Acceptance: Received January 16, 2014, and in revised form July 29, 2014. Accepted for publication September 13, 2014.

Correspondence: Address correspondence to Bram Stieltjes, MD, PhD, Im Neuenheimer Feld 280, DKFZ Heidelberg, Germany. E-mail: b.stieltjes@dkfz.de.

Financial Disclosures: All authors report no biomedical financial interests or potential conflicts of interest. This study has been partially funded by a Wings for Life grant.

*Shared corresponding authorship.

J Neuroimaging 2014;00:1-8.
DOI: 10.1111/jon.12202

Introduction

Spinal Cord Injury

Injury to the spinal cord often results in a devastating condition with the severe loss of motor, sensory, and autonomic functions. Substantial efforts have been made to obtain an effective therapy that could at least attenuate the outcome of spinal cord injury (SCI). Although some therapeutical approaches look promising;[1] generally, most of them prove to be ineffective. It is widely accepted that any intervention to improve the outcome of SCI should be administered early after the primary injury in order to prevent the secondary damage. An increasing amount of evidence indicates that erythropoietin (EPO) is an effective neuroprotective substance.[2–4] Recombinant human EPO is routinely used in patients with anemia of renal or tumor origin, but additionally, it has been reported to prevent secondary neuronal damage after experimental SCI[5] and stroke.[6] The mechanism of neuroprotective action of EPO appears to be based on several components: (1) an anti-ischemic effect, (2) anti-inflammatory capacity that reduces the extent of apoptosis, infiltration of proinflammatory cytokines and leukocytes, and (3) neoangiogenesis promoted by endothelial cell proliferation.[2] Apart from its neuroprotective effect, EPO has been shown to promote axonal regeneration.[7]

There are several morphological and functional approaches to assess the extent of tissue damage after SCI and the amount of spared tissue following application of various therapeutic strategies. Recently, manganese-enhanced magnetic resonance imaging (MEMRI) has been introduced in the arsenal of functional evaluation tests following experimental SCI in animal models.[8–11]

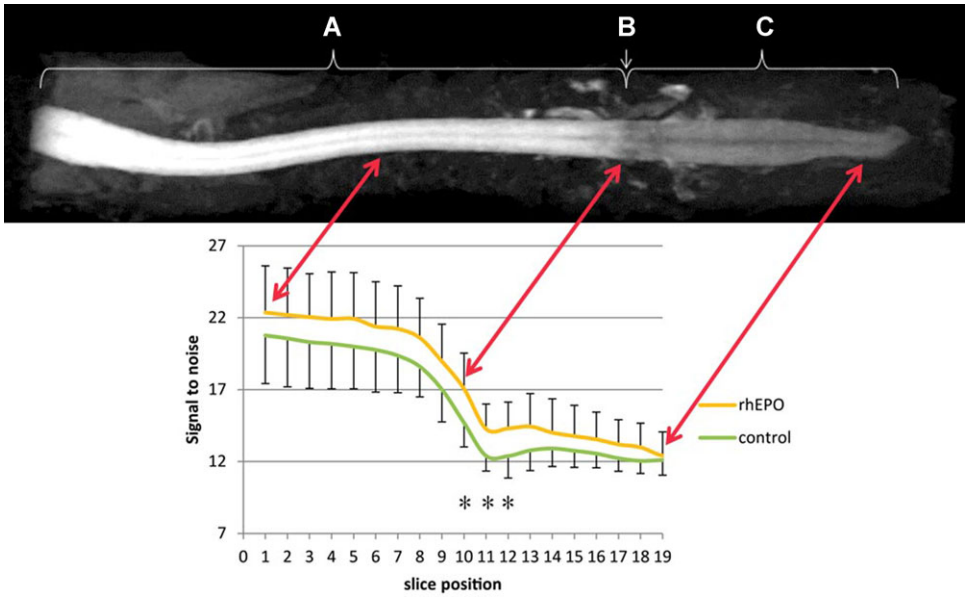

Fig 1. Upper part: postmortem T1-weighted manganese-enhanced magnetic resonance imaging of an extracted spinal cord (rat). The spinal cord has been stored and measured in a tube containing formaldehyde (A). Homogeneous contrast uptake is seen above the lesion epicenter (B). Below (C) a decrease of signal intensity is observed. Lower part: SNR within the spinal cord in the 2 groups. Slices are running from cranial (1) to caudal (19), the lesion epicenter was located at slice number 10. Error bars represent the standard deviation within both groups. The equivalent position of slice 1, 10, and 19 in the MEMRI is shown (see red arrows). Asterisks indicate significantly increased signal intensity in the EPO group compared to controls for slices 10 ($P = .031$), 11 ($P = .013$), and 12 ($P = .028$).

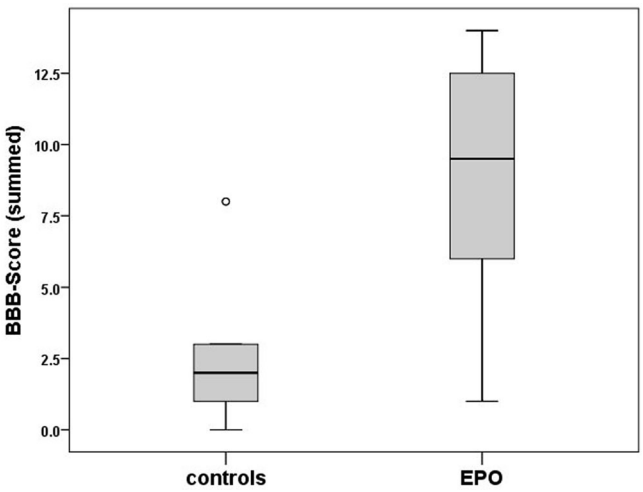

Fig 2. Boxplot distribution of functional examination (controls vs. EPO group on *x*-axis) using the BBB-score (*y*-axis); $n = 17$. The BBB-scores of both hind limbs have been summed to 1 value per animal. The EPO-treated animals show significantly higher values as a sign of therapy response ($P = .008$, $r = .62$) despite 2 overlapping outliers lying at value 8 in the control group.

Manganese-Enhanced Magnetic Resonance Imaging

Manganese was initially used as a radioactive tracer molecule in the central nervous system[12] and first introduced as a possible in vivo MRI contrast agent in 1998.[13] Mn^{2+}, analogue to Ca^{2+}, is taken up into neurons by voltage-gated Ca^{2+}-channels[14] and it is further transported along the axon.[12,15] Alternatively, Mn^{2+} is bound to transferrin and transported into the cell by endocytosis using the transferrin receptor.[16] The visualization of manganese is based on a strong contrast enhancement of Mn^{2+} ions in T1-weighted MRI, related to the shortening of the water spin-lattice relaxation time constant (T1).[13] Therefore, manganese acts as an excellent contrast agent for neuronal tissue when being imported and processed into the cell.[13] In general, the signal enhancement of the spinal cord in rats can be achieved after injecting Mn^{2+} into the cisterna magna.[17]

In a previous study, we have shown a close correlation of MEMRI results with locomotion testing and histology in rats undergoing SCI.[10] Therefore, we hypothesize that MEMRI is an adequate imaging-based evaluation method of therapy outcome in SCI. The aim of this study is to determine the short-term therapeutic effect of EPO after a spinal cord contusion injury in rats and compare MEMRI data with the results of locomotor tests and histological analysis.

Materials and Methods

Animals and Surgery

Experiments were carried out on 18 male Sprague-Dawley rats weighing 300-350 g (Animal Research Laboratories, Himberg, Austria) and lasted for a period of 3 days. The experimental protocol was approved in advance by the Animal Protocol Review Board of the City Government of Vienna. All procedures were carried out in full accord with the Helsinki Declaration on Animal Rights and the Guide for the Care and Use of Laboratory Animals of the National Institutes of Health (publication NIH 86-23, revised 1985). Rats were anesthetized by the intraperitoneal administration of a combination of ketamine hydrochloride + xylazine (ketamine hydrochloride:

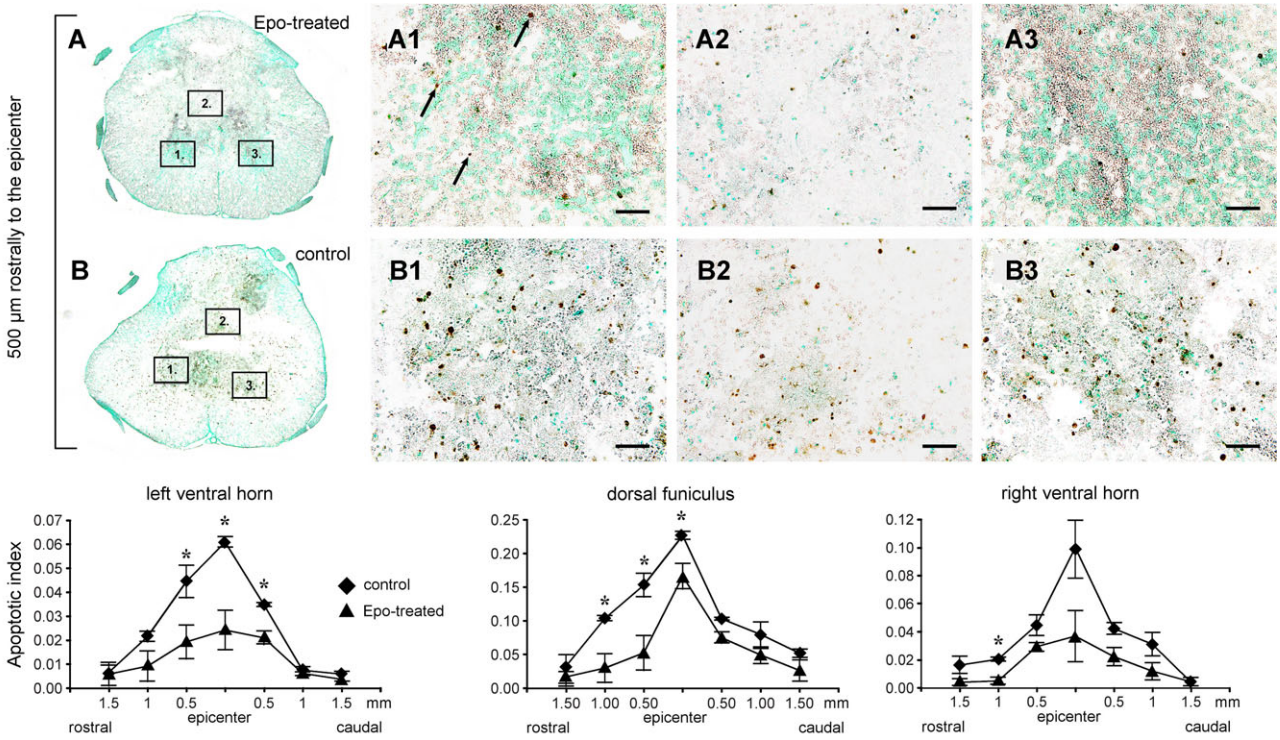

Fig 3. Immunohistological staining of apoptotic cells in the dorsal funiculus and in the left and right ventral horns of the spinal cord. Figures A1-A3 represent the EPO-treated group, B1-B3 the control group. Panels A and B show apoptotic cells indicated by their dark nuclei (arrows in A1). It is noted that fewer apoptotic cells occur in the spinal cords of rats treated with EPO (A1-A3) compared to controls (B1-B3). Graphs show the apoptosis index values at various levels cranially and caudally to the injury. Asterisks indicate significant difference between the EPO-treated and control group ($n = 4$ animals in each group), error bars indicate the standard deviation. Significant differences are found only cranially to the epicenter (*). Simple *t*-test, $P \leq .05$. Scale bar in A1-B3 = 50 μm.

90 mg/kg body weight, Ketavet, Pharmacia & Upjohn Co.; xylazine: 5 mg/kg body weight, Rompun, Bayer Co.). Animals received postoperative pain treatment immediately after the surgery (butorphanol tartrate; butorphanol, TEVA, 1.2 mg/kg body weight) and then a single daily dose of meloxicam (metacam, boehringer ingelheim, .75 mg/kg body weight) was administered for the next postoperative 3 days each. Adequate care was taken in all cases to minimize the levels of pain and discomfort during and after the operation. Core body temperature was measured with a rectal probe and maintained at 37°C. All rats underwent a laminectomy at the 11th thoracic vertebra (TH11) followed by a contusion injury using the infinite horizon impactor (Precision Systems and Instrumentation, LLC, Lexington, KY, USA). A definite impact force of 150 kdyn was used for the SCI ($n = 18$). The wound was closed by suturing according to anatomical layers. Postoperative treatment included subcutaneous injections of 10 ml Ringer's solution and antibiotics (Peni-Strepto, 50,000 IU, Virbac Laboratory, Carros, France) after surgery and then for 2 days.

After surgery, $MnCl_2$ injections were performed. Rats were fixed having their heads in a 90° flexed position and 80 μl of .8 mM $MnCl_2$ was administered via the atlanto-occipital membrane employing a 27-gauge needle. Animals in the EPO group ($n = 9$) received 1,000 IU/kg recombinant human EPO intravenously 1 hour after the injury, whereas animals in the control group ($n = 9$) received identical volumes of physiological saline.

At the end of the survival period, rats were reanesthetized as described above. The animals were first transcardially perfused with physiological saline containing 1,000 I.E. heparin (EBEWE Pharma, Unterach, Austria) followed by phosphate-buffered paraformaldehyde (4%, pH = 7.4, VWR International, Vienna, Austria). The vertebral column was removed postmortem from the 1st cervical to the 2nd sacral vertebra and immersion fixed overnight. After fixation, samples were stored in phosphate-buffered sucrose containing .01% Na-azide until processed for MRI analysis.

Locomotion Testing

The tester was blinded toward the group membership of the animals before surgery and 3 days after injury. Functional evaluation was based on the use of BBB-scoring, a locomotor rating scale originally introduced by Basso, Beattie, and Bresnahan (BBB-score).[18] In this test, the open field locomotion was examined separately on a scale from 0 to 21. The value 0 corresponds to total paraplegia of the hind limbs whereas the value 21 indicates fully intact locomotion. The rats were tested 1 day prior to surgery and all animals showed an intact locomotor pattern (score 21). All rats were euthanized after locomotion testing on day 3. One rat (EPO group) was excluded from functional recovery examinations due to testing difficulties.

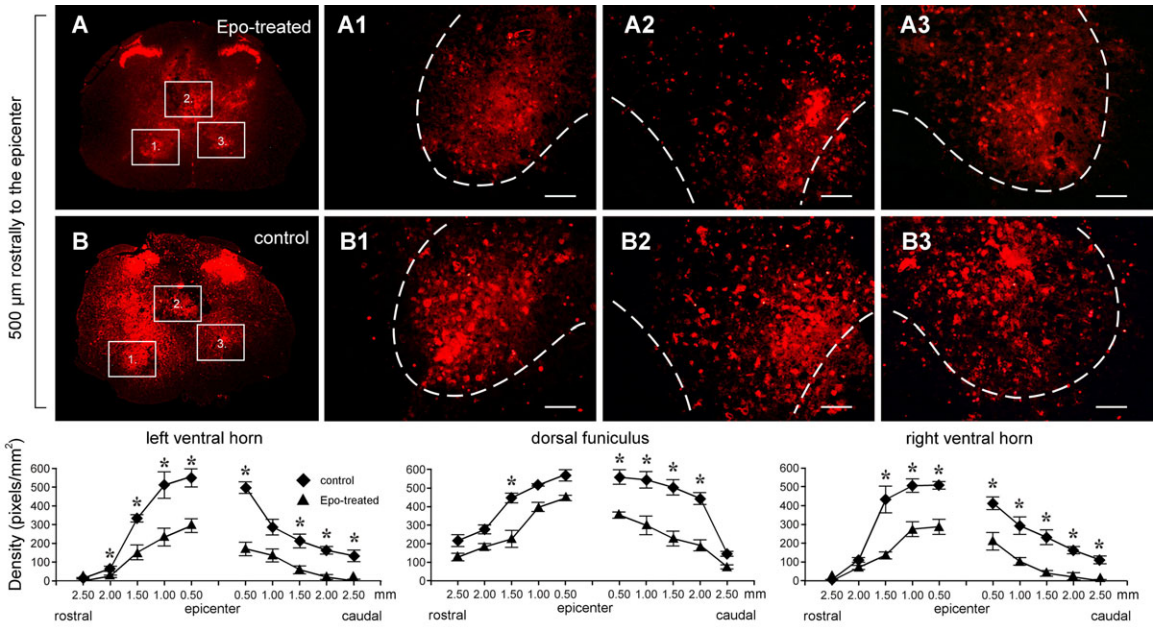

Fig 4. Microglia density measurements in the left ventral horn (A, A1 vs. B, B1), the dorsal funiculus (A, A2 vs. B, B2), and the right ventral horn (A, A3 vs. B, B3) of the spinal cord. The amount of microglia cells was significantly reduced in rats treated with EPO (A-A3) cranially and caudally to the lesion epicenter when compared to controls (B-B3). All images were taken .5 mm rostrally from the epicenter. Graphs show the microglial densities in the experimental groups. The dashed white lines indicate the border between gray (located within the lines) and white matter (located outside the lines). Error bars indicate the standard deviation. Simple *t*-test, $P \leq .05$. Scale bar in A1-B3 = 100 μm.

MRI

For the MRI examinations, the excised spinal cords were stored in tubes containing formaldehyde for fixation (15 ml capacity, 23 mm diameter). MRI was performed using a clinical 1.5-T-scanner (Siemens Symphony, Erlangen, Germany) with a custom-made animal volume resonator employing a T1-weighted 3-dimensional FLASH imaging pulse sequence (TR/TE 14.0/5.22 ms, voxel size in-plane .15 × .15 mm, 16 averages, flip-angle 30°, 28 partitions, partition thickness: .5 mm, field of vision 80 mm, matrix size 512 × 512, scan time 30 minutes). Imaging was performed perpendicular to the longitudinal axis of the spinal cord.

Image evaluation was performed using Syngo Via 25, included in the scanner software package (Siemens, Erlangen, Germany). The spinal cord was divided into 19 axial slices and slice 10 was placed at the height of the epicenter. Signal-to-noise ratio (SNR) was calculated on a region of interest-based method ($n = 18$). A region of interest was placed outside the animal contours for noise measurement. By taking the average of the most proximal and most distant noise measure, the SNR has been calculated. The 3-dimensional MRI reconstruction in Figure 5 was created using Fovia Software (Fovia Inc., Palo Alto, CA, USA).

Histological Assessment

After completing the MEMRI analysis of the samples, the spinal cords were carefully removed from the vertebral canal and immersed in 30% sucrose (in phosphate-buffered saline). In both the treatment and control groups, 5 animals were selected for evaluation that had the most uniform BBB values (ie, close to the mean BBB value in each group). The 25-μm-thick transverse parallel sections were cut on a cryostat (Leica CM 1850, Leica GmbH, Germany) and mounted onto gelatin-coated glass slides. The extent of apoptosis was assessed immunohistochemically using the ApopTag peroxidase in situ apoptosis detection kit S7100 (Merck Millipore Co, Billerica, MA, USA). This method labels the nucleosome-sized DNA fragments by tailing the 3'-OH ends of the fragments with digoxigenin deoxyribonucleotide triphosphate (dUTP) using terminal deoxynucleotidyl transferase (TdT). TdT catalyzes a template-independent addition of nucleotide triphosphates to 3'-OH ends of double- or single-stranded DNA. Endogenous peroxidase was inactivated by immersing the sections in 3% hydrogen peroxide. DNA fragments were then tailed with digoxigenin-dUTP by TdT, and incubated with an antidigoxigenin antibody conjugated with peroxidase for 30 minutes at room temperature. The reaction was visualized using diaminobenzidine and the sections were counterstained with methyl-green (VWR, Debrecen, Hungary).

In every spinal cord, a single section was investigated at the level of the epicenter and 2.5, 2, 1.5, 1, and .5 mm rostrally and caudally to that. Square areas of 250 μm × 250 μm in the ventral horns and in the ventral part of the dorsal funiculus were taken from microphotographs (Olympus FX50 epifluorescence microscope equipped with a DP70 digital camera) and digitally analyzed. The apoptotic index (AI), defined as the ratio of the total counted Apoptag-positive nuclei and the number of methyl-green-positive cells multiplied by 100 was determined by using the Image-J analysis program (NIH). Thus, the AI reflects the ratio of the apoptotic cells in the total number of cells in a given area of a spinal cord section ($n = 4$ for each area at each level).

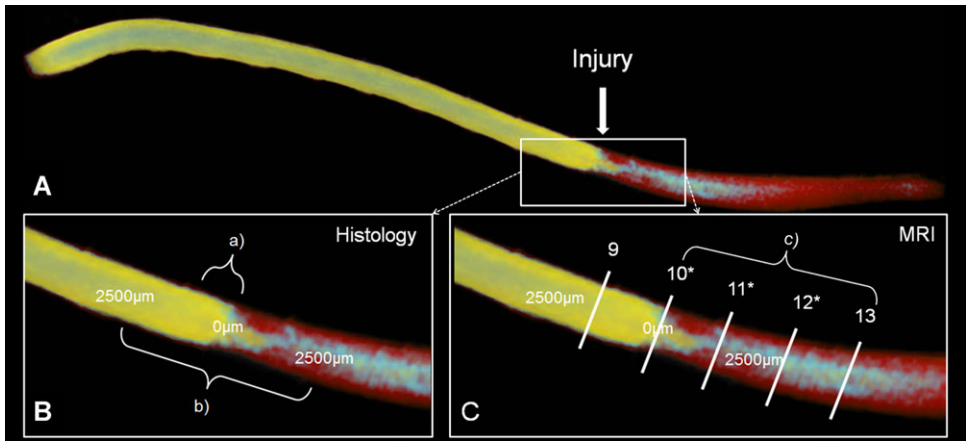

Fig 5. Three-dimensional MRI reconstruction of the spinal cord of a typical sample for the summarized presentation of findings. (A) Arrow: location of the injury which corresponds to slice 10 in every sample. The white rectangle indicates the magnified area of interest in the spinal cord. The cranial parts of the spinal cord show a clear, homogeneous uptake of manganese with high signal intensity (yellow color). Below the impact epicenter, a strongly reduced uptake of manganese is noticed (red color). Notably, there are centrally located areas below the impact zone which show an intermediate uptake of manganese (blue color). (B) To visualize the summarized changes of histological analysis, distances in micrometer from the epicenter are shown (0 and 2,500 μm, respectively). In the EPO group, there is a significantly decreased amount of apoptotic cells noticed (a) as well as a significantly decreased amount of microglia cells corresponding to the reduced immune response (b). (C) To demonstrate the correlating changes in signal intensity, distances in micrometer from the epicenter are shown. From left to right, slices 9-13 are plotted with white lines. Significantly increased signal intensity in the EPO group compared to controls was noticed for single slices 10 ($P = .031$), 11 ($P = .013$), and 12 ($P = .028$), indicated by asterisks, and also for the overall mean signal of slices 10-13 ($P = .017$; c).

Lectin histochemistry was performed on paralled cryostat section using biotinylated *Griffonia (Bandeira) simplicifolia* lectin B_4 (GSA-B_4, 1:200, overnight, Vector Labs, Burlingame, CA, USA). Lectin binding was visualized through the use of the streptavidin Alexa Fluor 546 conjugate (1:400, for 2 hours, Invitrogen). Fluorescent signals were detected in an Olympus FX50 epifluorescence microscope equipped with a DP70 digital camera (Olympus Ltd., Tokyo, Japan). Similar to the sampling method described above, square areas of 200 μm × 200 μm in the ventral horns and in the ventral part of the dorsal funiculus were digitally analyzed at the level of the epicenter and .5, 1.0, and 1.5 mm rostrally and caudally to the epicenter ($n = 4$ for each area at each level). Microglial densities indicated by the GSA-B_4 reaction were determined by using the Image-J analysis program (NIH).

Statistical Analysis

Statistics were performed using IBM SPSS Statistics Version 20.[19] We used an alpha level of .05 for all statistical tests. Linear regression of SNR (for all slices separately) and BBB-scoring was used with the group as independent variable to test the hypothesis regarding the difference between EPO and control group in MRI signal. To correlate MRI signal and BBB- scoring, Kendall's tau-b test was utilized. Simple student's *t*-test was used to analyze group differences of the microglial densities and the AI.

Results

MEMRI

EPO-treated animals showed higher SNR for slices 10-12 (slice 10: $P = .031$, $R^2 = .26$; slice 11: $P = .013$, $R^2 = .33$; slice 12: $P = .028$, $R^2 = .27$) located at the lesion epicenter. Slice 13 trended toward significance ($P = .08$, $R^2 = .126$). Also, mean SNR of slices 10-13 was significantly increased in EPO-treated animals ($P = .017$, $R^2 = .31$). A higher BBB-score correlated significantly with higher SNR values determined using the mean SNR between slices 10 and 13 ($P = .047$, $R^2 = .36$). The T1-signal of EPO-treated rats was overall increased compared to controls. The highest mean difference was noticed at slice 10 (~2.4 a.u.), which represented the lesion epicenter. As shown in Figure 1 and seen in every sample, the signal intensity continuously drops with a small slope from slice 1 to slice 7. Then, a higher slope is noticed between slices 7 and 11, representing the area around the lesion epicenter. Finally, the curve regains its original slope from the beginning, shown between slices 11 and 19 on the level of unenhanced spinal cord tissue as it has been reported earlier.[11]

Functional Evaluation

The BBB-scoring succeeded in 17 out of 18 rats ($n = 17$), 1 EPO-treated animal could not be analyzed. The results revealed a significant difference of BBB-scores between controls and treated animals ($P = .008$, $r = .62$). The box plot of distribution is shown in Figure 2. The functional examinations of the rats as quantified using the BBB-score showed significantly better outcome in the EPO group, however, with a higher variability represented by a more expanded distribution in the box plot graph (Fig 2). In contrast, the BBB-scores of the control group were in a more homogeneous, narrow range.

Histomorphological Findings and Comparison to MEMRI

Due to the short survival time, no proper cystic cavities were formed. Therefore, the morphological analysis focused on the

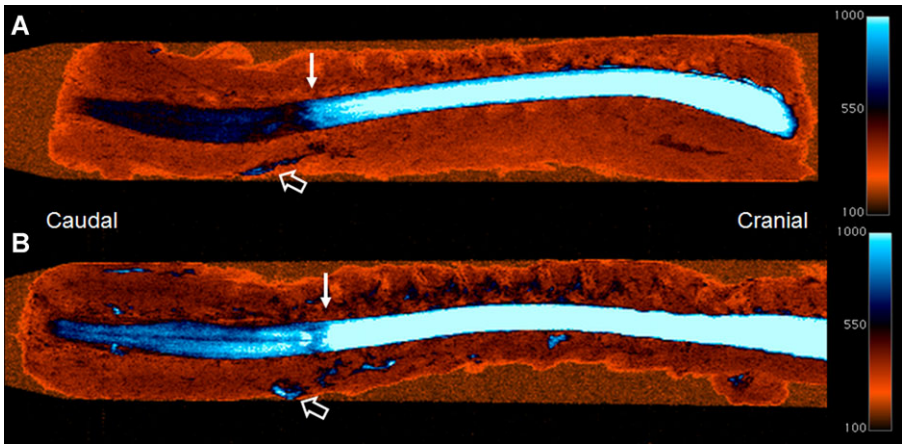

Fig 6. Color-coded signal intensity-based comparison of an untreated (A) and an EPO-treated animal (B) using the same window values. The untreated animal (BBB-score 1) shows lower uptake of manganese into the spinal cord (visible as blue color-coded stripe) caudally of the impact epicenter (white arrows) compared to the EPO-treated one (BBB-score 13). Lower signal intensity relates to reduced uptake of manganese. In this postmortem MEMRI, small manganese uptake may be found outside of the spinal cord (open arrow).

differences in the extent of apoptosis and microglial activity in the injured cord.

Significantly more apoptotic cells were found in the spinal cords of control animals at the epicenter and cranial to the lesion site at all 3 sampling sites (left and right ventral horns and ventral portion of the dorsal funiculus, Fig 3). The difference in AI between the control and the EPO-treated animals was negligible 1.5 mm cranially and 1 mm caudally to the epicenter. However, the greatest difference between the control and the treated groups were found in the region of the dorsal funiculus, where the main impact was implied to the cord.

Spinal cord segments affected in this region were densely populated by round, ameboid-like microglial cells, both in the control and the EPO-treated animals. However, microglial density was found to be upregulated to a much greater extent in the spinal cords of the control animals (Fig 4). Considerable microglial activation was observed in both the control and the EPO-treated cords 2 mm cranially and caudally to the epicenter (Fig 4). It is noted that microglial densities appeared to be moderate in the cords of EPO-treated animals caudally to the epicenter. Microglial densities at the level of epicenter were not determined due to the very high background noise. As shown in Figure 5, the significantly decreased apoptosis and immune reaction in the EPO group corresponded to the increased signal intensity. A comparison of an untreated and a treated animal is given in Figure 6.

Discussion

Findings of previous experimental in vitro and in vivo studies[9–19] suggest that 1) manganese preferably accumulates in healthy neuronal cells/axons, 2) damaged neurons show less contrast enhancement as a sign of less import of manganese into the cell and 3) locomotor assessment rating, histology results and Mn^{2+} concentrations correlate with MEMRI signal measurements. Taking the above listed arguments as basis for our current study, we hypothesized that MEMRI is an adequate tool for the monitoring of therapeutic approaches in SCI.

EPO Treatment Reduces Microglial Reactions and Apoptosis

Visualization of apoptotic cells in the injured cord showed significantly reduced numbers of apoptotic cells in EPO-treated animals compared to controls (Fig 3). The significant difference found in the dorsal funiculus rostral to the epicenter is thought to appear due to the degeneration of the ascending fibers in control animals. Microglia density measurements paralleled these results as EPO-treated animals had decreased microgliosis cranial and distal to the lesion epicenter than control animals, however, microglia densities were reduced all over the EPO-treated cords (Fig 4).

As reported earlier, the initial inflammation and later formed glial scar are perhaps the most important inhibitors of neural regeneration in SCI.[20] The invasion of microglia cells and leucocytes to the injury location is supposed to be an amplifier of inflammation since they themselves release proinflammatory/proapoptotic cytokines in the early spinal cord trauma.[21] Therefore, the number of microglia cells serves as an indicator for immune response and future outcome. In the very early phase of SCI, the initial homoeostasis of cytokines is disrupted by the trauma, followed by the upregulation of proinflammatory mediators, IL-1alpha/beta, IL-6 and TNF-alpha.[22] The release of these cytokines occurs 6 to 12 hours after the trauma and peaks at day 4.[22] All of these mediators are known to have cytotoxic abilities and may induce apoptosis. The molecular effects of EPO in SCI are yet not fully understood. As reported earlier, the binding of EPO to the EPO-R receptor on immune cells enhances the release of cell survival protein BcL-xL via JAK2/STAT5- and Nf-kb pathways[21] and therefore leads to reduced cell apoptosis. Upregulation of BcL-xL via JAK2/STAT3 and PI3K/AKT pathway activation by EPO may also have a neuroprotective effect on damaged neurons as it has been demonstrated for retinal neuron cells.[7] Both the limited extent of apoptosis and reduced microglial activation in EPO-treated animals is in line with other reports.[2]

A reduced number of apoptotic cells can clearly be considered to be a result of the neuroprotective effect of EPO. Also, the

reduced microglial activity in our samples is another sign of an indirect neuroprotective effect of EPO as robust microglial invasion eventually results in engulfing of degenerating neurons. Although this short-term study did not allow for the determination of the extent of regeneration in EPO-treated animals, it can be argued that limited microglial reactions induce less astroglial scarring and thus contribute to more extensive axonal regeneration in the EPO-treated spinal cords.[20] Thus, together with earlier reports,[3,7] our results support the dual function of EPO therapy promoting both regeneration and neuroprotection in the central nervous system.

MEMRI and Functional Recovery

We found a significantly increased overall T1-signal in EPO-treated animals (Fig 1). The SNR values around slice 10 – the impact epicenter – reveal the highest differences in T1 signal (~2.4 a.u.) thus indicating that the highest difference in healthy neurons between the 2 groups can be found there. It was hypothesized that MEMRI will depict a loss of T1w contrast that is partially reversible under EPO therapy in SCI. In accordance with this hypothesis, overall, higher T1 signal in EPO-treated animals indicates a higher number of healthy neurons which are able to uptake manganese as a sign of vital function. Substantiating this observation, BBB-score and SNR showed good correlation indicating that a higher SNR between slices 10 and 13 corresponded to a higher physical examination value, independent of the group. Comparing the physical examinations of both groups, we assume that EPO therapy significantly increases the functional recovery in rats after 3 days after injury and that there are individual differences in response to EPO therapy which explains the broadening of the distribution. In summary, our histological, functional findings and the imaging-based evaluation support a neuroprotective and also a secondary regenerative effect of EPO in early SCI. Moreover, MEMRI is an adequate method for the EPO therapy evaluation as it indicates the amount of damaged neurons in a semiquantitative approach.

An interesting, yet unsolved, question is why a reduced manganese contrast enhancement is also seen above the lesion epicenter (Fig 1, slices 6-9, this result was already found in a previous study[11]). As the loss of a neuron is also accompanied by the loss of its axon and its integration in a complex neuronal network, it seems to be plausible that the injury also affects neuronal cells on other levels. A suitable explanation for this effect is that the missing contrast enhancement above the epicenter results from the complete disconnection of axons at the height of the traumatic injury which then leads to a decreased uptake of manganese above the lesion. This thesis also supports the finding that the signal intensity below the epicenter corresponds to that of a nonenhanced spinal cord, caused by the irrevocable destruction of axons.

An uncertain factor is the potential manganese uptake by microglial cells. There is evidence that microglial cells have voltage-gated Ca^{2+} receptors at the cell surface albeit they seem to play a less important role under normal conditions.[21,22] Thus, microglial cells may take up manganese, similar to the uptake in neuronal tissue. In this case, the loss of signal due to neuronal damage could be counteracted by the increase of microglia invasion at the injury site. However, the calcium current in microglial cells is small and not observed under physiological conditions[22] and thus presumably contributes, if at all, to a minor extent to MEMRI.

The histology results correlated well to the findings obtained by MEMRI. We believe, that the reduced amount of apoptotic cells is the main reason for the increased T1-signal intensity in EPO-treated animals as it has been analogously already reported earlier.[9,11]

One limitation of the study is that the physical examination was performed in vivo, whereas MRI quantification was performed ex vivo, analogously to earlier reports. Thus, after the extraction and fixation of the spine, Mn^{2+} may have diffused from the neuronal tissue into the surrounding tissue. We know from earlier studies,[8,10,11] that Mn^{2+} is preferably taken up by healthy neurons but this diffusion process may decrease the initial in vivo difference in signal intensity to the disadvantage of treated animals. However, we did not observe a signal increase in the surrounding tissue and found a significant difference between the 2 groups postmortem. We cannot exclude a diffuse loss of Mn^{2+} and assume that the group difference may be even larger if the experiment is performed in vivo.

Summary and Conclusion

We investigated rats with SCI 3 days after injury and therefore, our study serves as a model for the initial stage of the trauma. In this short-term evaluation, we show that the intravenous application of EPO leads to a significant better recovery after SCI in rats at 3 days and that MEMRI may serve as a semiquantitative imaging approach to monitor the response of damaged neuronal tissue to EPO therapy.

References

1. Casha S, Zygun D, McGowan MD, Yong VW, Hurlbert RJ, et al. Results of a phase II placebo-controlled randomized trial of minocycline in acute spinal cord injury. *Brain* 2012;135:1224-1236.
2. Lombardero M, Kovacs K, Scheithauer BW. Erythropoietin: a hormone with multiple functions. *Pathobiology* 2011;78:41-53.
3. Sargin D, Friedrichs H, El-Kordi A, et al. Erythropoietin as neuroprotective and neuroregenerative treatment strategy: comprehensive overview of 12 years of preclinical and clinical research. *Best Pract Res Clin Anaesthesiol* 24:573-594.
4. Marti HH, Bernaudin M, Petit E, et al. Neuroprotection and angiogenesis: dual role of erythropoietin in brain ischemia. *News Physiol Sci* 2000;15:225-229.
5. Kaptanoglu E, Solaroglu I, Okutan O, et al. Erythropoietin exerts neuroprotection after acute spinal cord injury in rats: effect on lipid peroxidation and early ultrastructural findings. *Neurosurg Rev* 2004;27:113-120.
6. Wang L, Zhang Z, Wang Y, et al. Treatment of stroke with erythropoietin enhances neurogenesis and angiogenesis and improves neurological function in rats. *Stroke* 2004;35:1732-1737.
7. Kretz A, Happold CJ, Marticke JK, et al. Erythropoietin promotes regeneration of adult CNS neurons via Jak2/Stat3 and PI3K/AKT pathway activation. *Mol Cell Neurosci* 2005;29:569-579.
8. Bilgen M, Dancause N, Al-Hafez B, et al. Manganese-enhanced MRI of rat spinal cord injury. *Magn Reson Imaging* 2005;23:829-832.

9. Martirosyan NL, Bennett KM, Theodore N, et al. Manganese-enhanced magnetic resonance imaging in experimental spinal cord injury: correlation between T1-weighted changes and Mn(2+) concentrations. *Neurosurgery* 2010;66:131-136.
10. Walder N, Petter-Puchner AH, Brejnikow M, et al. Manganese enhanced magnetic resonance imaging in a contusion model of spinal cord injury in rats: correlation with motor function. *Invest Radiol* 2008;43:277-283.
11. Stieltjes B, Klussmann S, Bock M, et al. Manganese-enhanced magnetic resonance imaging for in vivo assessment of damage and functional improvement following spinal cord injury in mice. *Magn Reson Med* 2006;55:1124-1131.
12. Sloot WN, Gramsbergen JB. Axonal transport of manganese and its relevance to selective neurotoxicity in the rat basal ganglia. *Brain Res* 1994;657:124-132.
13. Pautler RG, Silva AC, Koretsky AP. In vivo neuronal tract tracing using manganese-enhanced magnetic resonance imaging. *Magn Reson Med* 1998;40:740-748.
14. Narita K, Kawasaki F, Kita H. Mn and Mg influxes through Ca channels of motor nerve terminals are prevented by verapamil in frogs. *Brain Res* 1990;510:289-295.
15. Pautler RG, Mongeau R, Jacobs RE. In vivo trans-synaptic tract tracing from the murine striatum and amygdala utilizing manganese enhanced MRI (MEMRI). *Magn Reson Med* 2003;50:33-39.
16. Aschner M, Aschner JL. Manganese neurotoxicity: cellular effects and blood-brain barrier transport. *Neurosci Biobehav Rev* 1991;15:333-340.
17. Liu CH, D'Arceuil HE, de Crespigny AJ. Direct CSF injection of MnCl(2) for dynamic manganese-enhanced MRI. *Magn Reson Med* 2004;51:978-987.
18. Basso DM, Beattie MS, Bresnahan JC. A sensitive and reliable locomotor rating scale for open field testing in rats. *J Neurotrauma* 1995;12:1-21.
19. IBM. SPSS Statistics. *Release* 20:2011.
20. Leal-Filho MB. Spinal cord injury: from inflammation to glial scar. *Surg Neurol Int* 2011;2:112.
21. Moller T. Calcium signaling in microglial cells. *Glia* 2002;40:184-194.
22. Colton CA, Jia M, Li MX, et al. K^+ modulation of microglial superoxide production: involvement of voltage-gated Ca^{2+} channels. *Am J Physiol* 1994;266:C1650-C1655.